

# Preservicing Mission, On-Orbit Modifications to Hubble Space Telescope Pointing Control System

G. S. Nurre\* and J. P. Sharkey†

NASA Marshall Space Flight Center, Alabama 35812

J. D. Nelson‡

Lockheed Missiles and Space Co., Inc., Sunnyvale, California 94089

and

A. J. Bradley§

Allied Signal Aerospace Co., Annapolis, Maryland 20701

Because of unexpected, thermally induced disturbances originating in the solar arrays (SAs), the Hubble Space Telescope was initially unable to meet its pointing error specifications of 0.007 arc-s [root mean square] for observations lasting from a few seconds to several hours. The effort to pinpoint the mechanism causing the problem and to redesign the onboard controller to accommodate the disturbance began shortly after deployment. After controller modifications, the pointing errors were well within the specification for all of the orbit except for short intervals during transitions in and out of Earth's shadow. This paper presents a chronology of the redesign process and flight data showing the achieved pointing performance. During the recent servicing mission (December 1993) the SAs were replaced with arrays of a modified mechanical design. A preliminary assessment of pointing performance since that time is presented.

## Introduction

THE Hubble Space Telescope (HST) was designed and built under the direction of Marshall Space Flight Center and is composed of the systems support module, built by Lockheed Missiles & Space Company, the optical telescope assembly, built by Hughes Danbury Optical Systems, the solar arrays (SAs), furnished by the European Space Agency, and five science instruments, developed and delivered under the management of Goddard Space Flight Center (GSFC). HST is operated under the direction of GSFC. The HST is an orbiting, 2.4-m-diam Ritchie-Cretien-type Cassegrainian telescope, having resolving capability of approximately 0.5 arc-s, that is operated as an international astronomical observatory.<sup>1</sup> Launched on the orbiter *Discovery* on April 25, 1990, it was deployed the next day with the remote manipulator system in a 611-km circular orbit. Prior to release the two (SAs) and the two high-gain antennas (HGAs) were deployed. The HST was released with the SAs and  $-V_1$  axis oriented toward the sun. After a 3-min interval, which allowed the orbiter to back away, the sun pointing mode was autonomously engaged to point the  $-V_1$  axis at the sun. Figure 1 shows the coordinate reference frame and the major elements of the HST. The process of defining an attitude reference was carried out; once the aperture door was opened, 42 h after release, the transition to the normal operational mode was begun. Unlike the problem with the primary mirror, which took weeks to verify, it was immediately obvious from observing real-time data that there were unexpectedly large perturbations in the pointing control system (PCS). There immediately began a concerted effort to determine the source of the disturbance and to consider modifications to the onboard control laws that might bring the PCS back within specification. As it was quickly learned that the SAs were at the root of the problem, the modified control system architecture came to be known as the PCS solar array gain augmentation (SAGA). This paper gives a chronology of the design changes leading to the final preservicing mission

controller that meets a revised specification. Although emphasis is placed on the current design and its associated performance, an overview of the originally baselined design, a description of the origins of the SA disturbance, and a brief sketch of the early phases of the SAGA redesign are included.

## Pointing Control System Requirements, Baseline Design, and Initial Performance

The original pointing requirement for the HST was to maintain an image on the focal plane stable to 0.007 arc-s (rms) for observations lasting from 10 s to 24 h. A derived requirement associated with the design of the fine guidance sensors (FGSs), three star trackers in the focal plane of the optical telescope assembly (OTA), required that the FGSs not lose lock on their guide stars (GSs), a condition denoted as loss of lock. In consideration of the present disturbance environment and the practical needs of the science instruments, the pointing requirements have been redefined as follows. For 95% of all 1-min intervals during an orbit the total pointing error will be less than 0.007 arc-s (rms), the error for any 1-min period shall not exceed 0.012 arc-s (rms), and loss of lock shall not occur more often than once every 16 orbits.

The HST PCS is composed of four reaction wheels assemblies (RWAs), three or four of six reference gyros, three FGSs, and a fixed-point, 24-bit flight computer. There is a magnetic momentum management system that continuously unloads the wheels, sun sensors used in coarse attitude determination and safemode, and three NASA standard star trackers used for attitude updates to insure GS acquisitions. The control system algorithm is computed at 40 Hz and contains proportional-integral-derivative (PID) terms. References 2 and 3 can provide extensive detail on the baseline PCS, and Ref. 4 explains the design and operation of the FGS.

The pointing performance for the baseline PCS was, for the most part, dismal and was a long way from meeting the pointing requirements. Large errors exceeding 0.1 arc-s occurred at terminator crossings, and somewhat smaller but still significant perturbations were prevalent throughout the orbit. The one consistent exception was the period 10–12 min prior to entry into night when the pointing was very good, approximately 0.003 arc-s rms. This was an encouraging piece of information, for it indicated that, when the disturbance was absent, the PCS [RWAs and rate gyro assemblies (RGAs)] were well behaved. A more thorough analysis of the base-

Received Oct. 26, 1993; revision received March 10, 1994; accepted for publication Sept. 4, 1994. This paper is declared a work of the U.S. Government and is not subject to copyright protection in the United States.

\*Chief Scientist, Structures and Dynamics Laboratory/ED01.

†Deputy Chief, Precision Pointing Systems Branch/ED12, Structures and Dynamics Laboratory.

‡Group Engineer, Organization 74-16, Bldg. 580, 1111 Lockheed Way.

§Chief Engineer, HST Pointing Control System, P.O. Box 91.

line system performance can be found in Refs. 5 and 6. Clearly the evidence indicated that the origin of the perturbation was a thermally driven excitation of some part of the structure.

Analysis of the large quantity of data that was collected over several months of operation strongly implicated the SAs as the source of

the pointing perturbations. The details of that investigation together with a technical description of the mechanisms and dynamics of the SAs can be found in Refs. 6 and 7. To summarize the results, it was determined that the disturbance spectrum was dominated by the out-of-plane and in-plane modes of the SA, having frequencies of 0.11 and 0.65 Hz, respectively. The excitation of the SA modes was caused by thermal deformations and the storing and releasing of energy in the mechanisms.

### Control System Redesign: SAGA

Since there was no chance of eliminating the disturbance at its source, it was understood from the very beginning that the sole means of reducing the effects of the disturbance was by way of a modification to the controller software. The flight data clearly showed the required disturbance attenuation at the dominant SA frequencies, and so it was a matter of reshaping the disturbance rejection transfer function to achieve this. Because the new controller would require the development of new software (not simply modifications to existing constants) and because of the time required to develop and verify flight software, the architecture of the new controller was selected before the design was done. Thus, two sixth-order filters,  $G_A$  and  $G_F$ , were introduced in each axis, as shown in Fig. 2. It was decided that the disturbance attenuation would be done

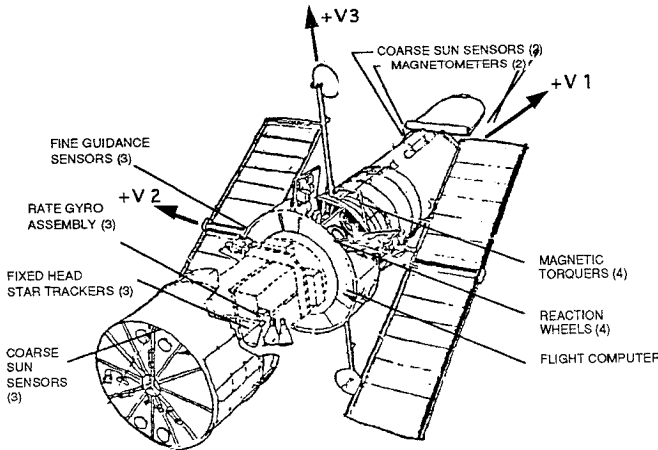


Fig. 1 Hubble Space Telescope.

Table 1 HST dynamics models: prelaunch and measured on-orbit

Mode	Description	Prelaunch model				Postlaunch model				
		Frequency, Hz	$V_1$	$V_2$	$V_3$	Frequency, Hz	$\zeta$	$V_1$	$V_2$	$V_3$
1	SA out of plane	0.086	0.056	0.0	0.025	0.114	0.010	0.056	0.018	0.025
2	SA out of plane	0.087	0.0	0.018	0.0	0.120	0.010	0.056	0.018	0.025
3	HGA	0.432	0.0	0.012	0	0.432	0.006	0	0.012	0
4	SA in plane	0.462	0.0	0.0	0.079	0.630	0.006	0	0	0.079
5	SA in plane	0.710	0.211	0.0	0	0.710	0.006	0.211	0	0
6	HGA	0.713	0.016	0.0	0	0.713	0.006	0.016	0	0
7	Aperture door	0.912	0.0	0.057	0	0.912	0.006	0	0.057	0
8	Solar array	1.041	0.087	0.0	0	1.041	0.006	0.087	0	0
9	Solar array	1.079	0.0	0.0	0.029	1.079	0.006	0	0	0.029
10	HGA	1.155	0.094	0.0	0	1.155	0.006	0.094	0	0
11	Solar array	2.508	0.0	0.0	0.013	2.508	0.006	0	0	0.013
12	Solar array	2.729	0.040	0.0	0	2.729	0.006	0.040	0	0
13	HGA	2.816	0.015	0.0	0	2.816	0.006	0.015	0	0
14	HGA	2.863	0.059	0.0	0	2.863	0.006	0.059	0	0
15	Solar array	4.271	0.020	0.0	0	4.271	0.006	0.020	0	0
16	Aperture door	10.834	0.048	0.024	0.104	10.834	0.007	0.048	0.0240	0.104
17	Aperture door	12.133	0.030	0.155	-0.320	12.133	0.007	0.030	0.155	-0.320
18	Pitch scissors	13.201	-0.018	-1.341	-0.110	13.201	0.007	-0.018	-1.341	-0.110
19	Aperture door	14.068	0.0	-1.387	-0.217	14.068	0.006	0	-1.387	-0.217
20	Yaw scissors	14.285	0.030	-0.806	-1.516	14.285	0.007	0.030	-0.806	-1.516
21	Aperture door	15.264	0.076	-0.134	0.170	15.264	0.006	0.076	-0.134	0.170
22	Wide Field/Planetary Camera, OTA	18.915	-2.161	0.0	0	18.915	0.011	-2.161	0	0
23	RWA Isolators	19.315	-16.79	0.0	0	19.315	0.040	-16.792	0	0

Note: Principal moments of inertia ( $\text{kg m}^2$ ):  $I_{11} = 31,046$ ,  $I_{22} = 77,217$ ,  $I_{33} = 78,754$ ; critical damping ratio  $\zeta = 0.005$  for all prelaunch modes.

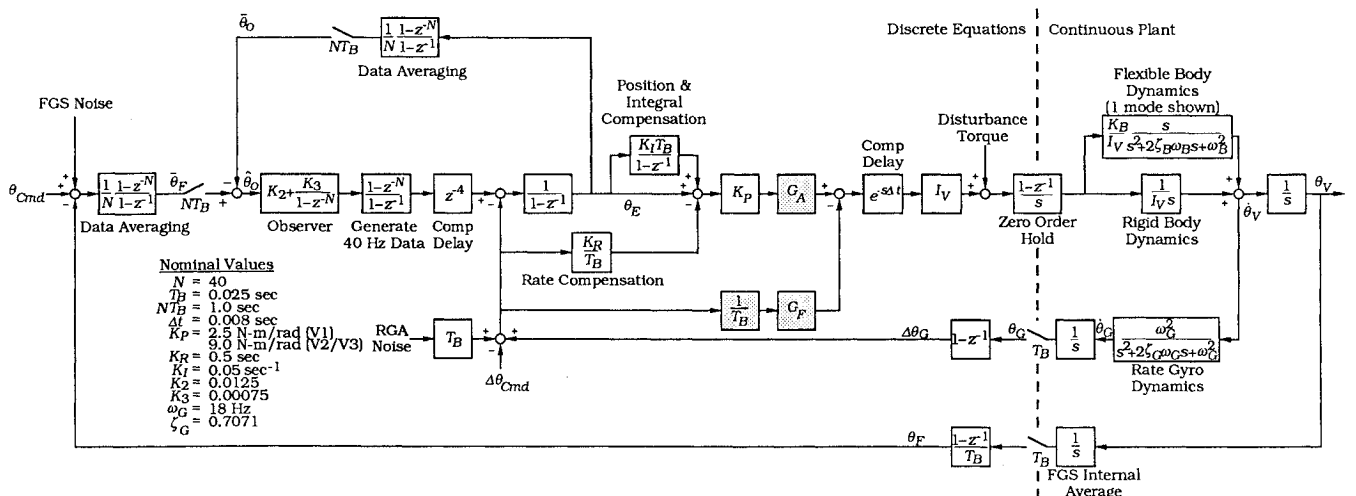


Fig. 2 Simplified PCS block diagram.

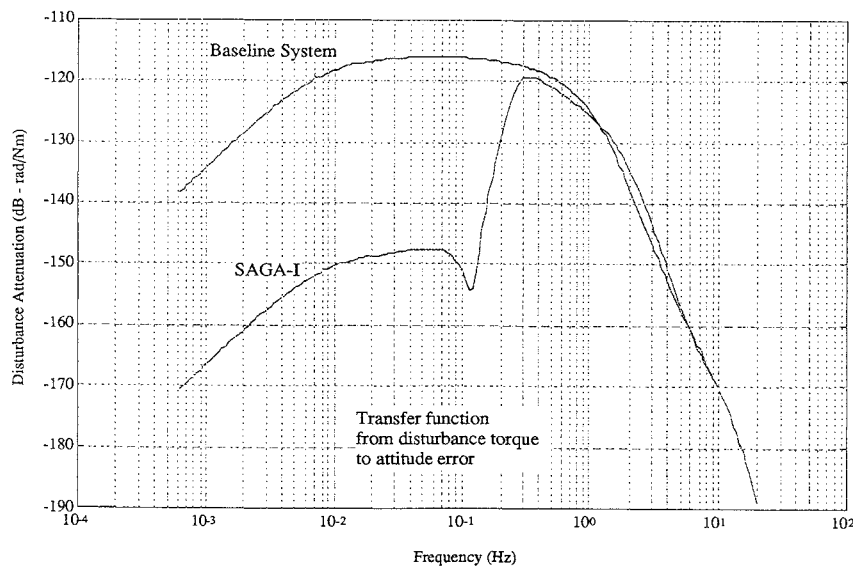


Fig. 3 Disturbance rejection characteristics for baseline controller and for SAGA-I.

in phases beginning by adding attenuation at the first mode of the SA and then proceeding to higher frequency modes. The entire process was done in three phases, SAGA-I, SAGA-GA, and SAGA-II. The control design and the resulting pointing performance associated with each phase are described in the following paragraphs. Midway through the redesign activity it became apparent that, in order to get the most performance from the constrained system, a more accurate model of the structural modes was required. An abbreviated on-orbit dynamics test was performed<sup>8</sup> and resulted in the postlaunch modes shown in Table 1. The new software was to be designed so that the baseline controller could be reinstated by ground command, and all of the original safemode functions were to be operational as in the baseline. Many of the details of what follows can be found in Ref. 9.

### SAGA-I

SAGA-I was the initial attempt at modifying the control law to reduce the adverse effects of the SA disturbance. Details of the design and performance of SAGA-I have been published in Refs. 5 and 6 and are briefly summarized here so that more space can be devoted to the more recent activities. The intent in undertaking SAGA-I was to attenuate by a factor of at least 30 the disturbance component at the first SA mode (0.11 Hz). The  $G_F$  was designed to provide acceleration feedback with a large gain at that frequency, and  $G_A$  was selected to maintain the original PID characteristics of the outer loop, since there was evidence to indicate that the PID controller had good response characteristics and stability margins. The disturbance rejection characteristics for both the baseline system and for SAGA-I are shown in Fig. 3.

SAGA-I was tested during a 12-h period in October 1990 with mixed results. The required attenuation at the first SA mode was achieved, but during intervals of elevated disturbance certain variables in the controller software were driven into their limits, resulting in limit cycles and safemode entries.

The SAGA-I controller, although not entirely a success, did point the way to the design of the next SAGA phases.

### SAGA-GA

Although the original SAGA design was reasonably successful, nonlinear performance due to the dynamic range limitations imposed by the fixed-point flight computer caused the team to develop a modified design that used only one of the two sixth-order filters, the GA filter (Fig. 4). This system became known as SAGA-GA. SAGA-GA uses the original SAGA architecture, but it incorporates different database coefficients to modify the filter characteristics. The sensitivity to saturations was reduced by eliminating the high gain at low frequencies. The GF filter was effectively removed by setting the filter database coefficients and input and output limiters

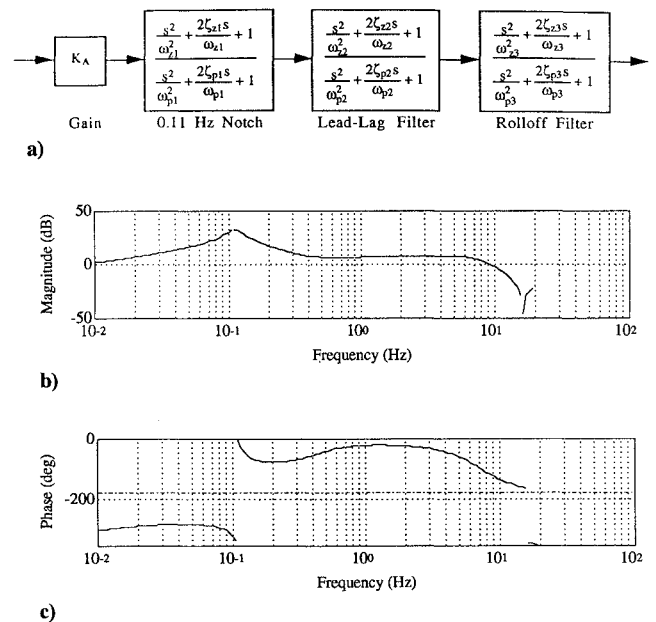


Fig. 4 GA filter block diagram and transfer function for SAGA-GA.

to zero. The design goal for SAGA-GA was to attenuate the disturbances due to the 0.11-Hz SA modes by at least a factor of 30 while maintaining system stability and improving robustness with respect to nonlinear effects.

### SAGA-GA Design

SAGA-GA design reflects several "lessons learned" from the original SAGA. First, the direct-current (dc) gain was lowered. A high dc gain is normally desirable to improve transient performance. However, if the high gain causes the system to reach nonlinearities, it may degrade performance. This was seen in the original SAGA testing. Next, the peak of the GA magnitude (translates into disturbance attenuation) was reduced to 35 dB. Data analysis from the original SAGA testing showed that a factor of 30 attenuation on the 0.1-Hz modes would be sufficient. This change also made it easier to produce a stable system. Third, the proportional gain was shifted as much as possible from the PID block to the GA filter to allow maximum GA filter inputs without saturation, so a maximum filter dynamic range could be attained. Finally, the GA filter in the SAGA-GA design has a gain above 8 dB out to 5 Hz. This was done to increase attenuation of higher frequency modes, especially the 0.65-Hz mode, since early SAGA testing

showed the 0.65-Hz mode to be a significant contributor to the total jitter.

The components of the GA filter are shown schematically in Fig. 4 in continuous form. Elements include a gain term, a second-order term to produce a peak at 0.11 Hz, a lead-lag term for stabilization, and a second-order filter for high-frequency rolloff.

Figure 4 shows a Bode plot of the  $G_A V_3$  axis filter for the SAGA-GA design. Characteristics of note include a low-frequency gain

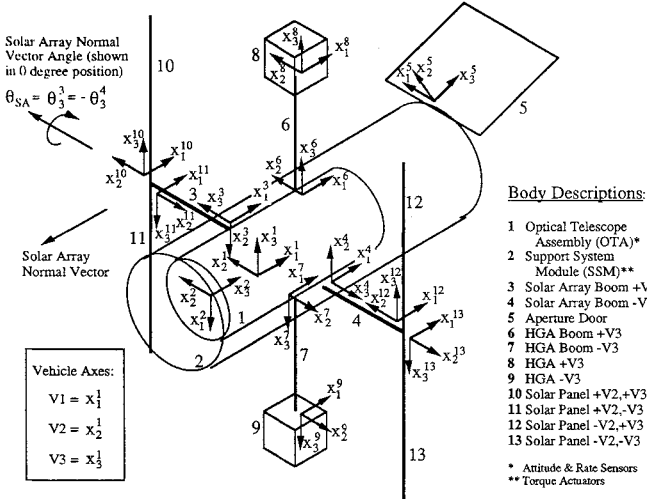


Fig. 5 HST multibody dynamic model used in performance simulations.

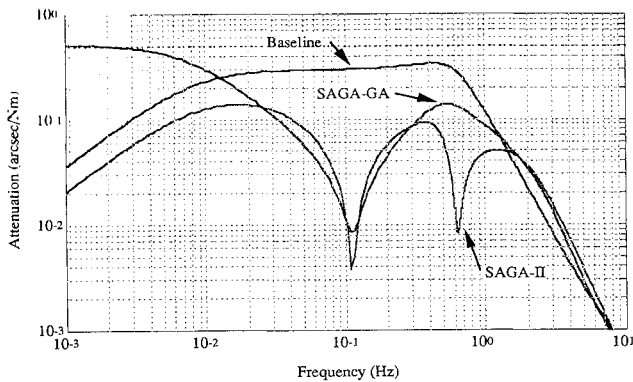


Fig. 6 Disturbance rejection characteristics for baseline, SAGA-GA, and SAGA-II controllers.

near  $-1.5$  dB, a peak of 35 dB at 0.11 Hz, positive gain of approximately 8 dB at 0.6 Hz, and high-frequency rolloff above 5 Hz.

The open-loop gain crossover frequency is an indicator of closed-loop bandwidth. Table 2 shows these crossover frequencies for the baseline PID, SAGA-GA, and SAGA-II systems without bending modes. Improved knowledge of HST modal parameters obtained through on-orbit testing allowed further increases in bandwidth for the SAGA-II system (next section).

From the block diagram (Fig. 2), using the approximation  $|(1/s)G_{PID}| \gg 1$ , relative attenuation of disturbance torques between the baseline PID and SAGA-GA is seen to be

$$\frac{(\theta_v/T_D)_{BL}}{(\theta_v/T_D)_{SAGA-GA}} \approx GA \frac{K_{P,SAGA-GA}}{K_{P,BL}} \quad (1)$$

where  $K_P$  is included since the gains have been adjusted to shift as much gain as possible into the GA filter.

Figure 6 shows  $V_3$  disturbance rejection results for SAGA-GA along with the baseline PID results. As expected, the difference between the baseline curve and the SAGA-GA curve on  $V_3$  corresponds with the magnitude plot of the GA filter (Fig. 4) scaled by the ratio of the baseline PID and the SAGA-GA proportional gains (9.9 and 5.561, respectively) in the frequency range 0.01–0.5 Hz.

A major concern during design of the SAGA-GA system was the nonlinear operation of the filter. Careful limiter selection was performed to reduce nonlinear effects. Limiters were selected so the system would degrade gracefully when in the nonlinear regime, as was likely to occur at terminator crossings. Limiters were chosen to limit maximum torque command on each axis and allow filter dynamics to have maximum possible range to compensate for the 0.11-Hz disturbance.

Extensive checkout was performed through the use of a high-fidelity simulation prior to on-orbit testing. The simulation incorporates a 13-body dynamic model including the SAs (Fig. 5) as well as a SA terminator disturbance model. In addition, all control laws and control system hardware (reaction wheels, gyros) are simulated. Simulation runs confirmed analysis results

Table 2 Comparison of open-loop gain crossover frequencies for baseline, SAGA-GA, and SAGA-II controllers

Axis	Frequency, Hz		
	Baseline PID	SAGA-GA	SAGA II
$V_1$	0.30	0.66	1.06
$V_2$	0.66	1.3	1.83
$V_3$	0.66	1.3	1.83

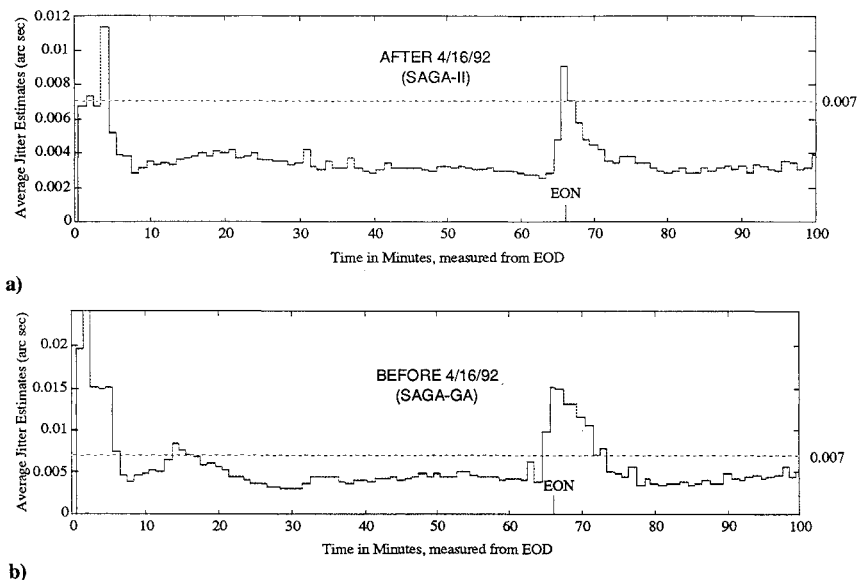


Fig. 7 HST pointing stability performance for SAGA-GA and SAGA-II.

that showed significant jitter reduction and improved loss of lock performance. Simulation work was also used to validate the limiters.

### SAGA-GA On-Orbit Results: April 3, 1991 to April 16, 1992

After a successful test on March 30, 1991, the SAGA-GA software was turned back on for normal operations on April 3, 1991. SAGA-GA remained in operation until the SAGA-II system was installed permanently on April 16, 1992. SAGA-GA performance was as predicted. Time- and frequency-domain results demonstrated attenuation near a factor of 30 in the dominant 0.11-Hz mode. In addition, attenuation of a factor of 2 was obtained on the 0.65-Hz mode. Oscillations at terminator crossings were substantially reduced, so settle time at a crossing was reduced from 6–7 to 3–4 min and nonlinear operation of the control system was nearly eliminated. Pointing errors caused by midday disturbances were reduced. As a result, the jitter level was below 0.007 arc-s approximately 85% of each orbit, compared to 42% with the baseline PID control system. Figure 7 shows long-term SAGA-GA performance data, along with similar data for SAGA-II. These calculations are based on 1-min averaging and show that the 0.007-arc-s specification is exceeded approximately 15 min out of an orbit during periods near terminators.

Figures 8 and 9 illustrate the performance improvement on the  $V_2$  axis with SAGA-GA and the baseline PID system (SAGA-GA off) at an enter orbit night (EON) terminator. The  $V_2$  SAGA-GA-off case is dominated by 0.11-Hz modes and shows substantial energy at 0.4 and 0.6 Hz, whereas the SAGA-GA-on case is dominated by 0.65-Hz modes.

Loss of lock performance also improved considerably with SAGA-GA. Smaller body rates and attitude errors due to improved disturbance attenuation reduced instances of fine lock. Prior to

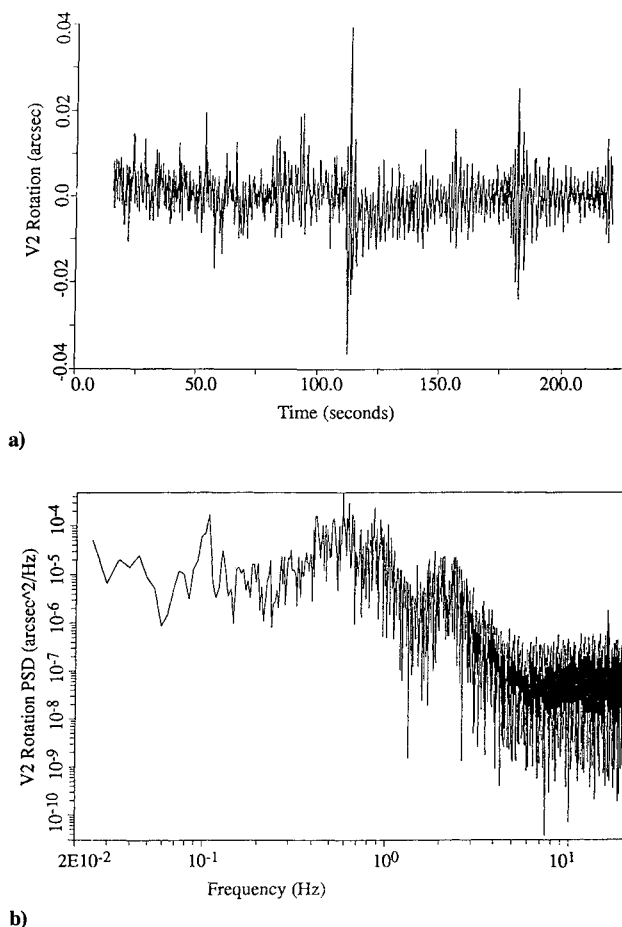


Fig. 8 The  $V_2$  axis pointing error time history and corresponding power spectral density for SAGA-GA controller in gyro hold at EON.

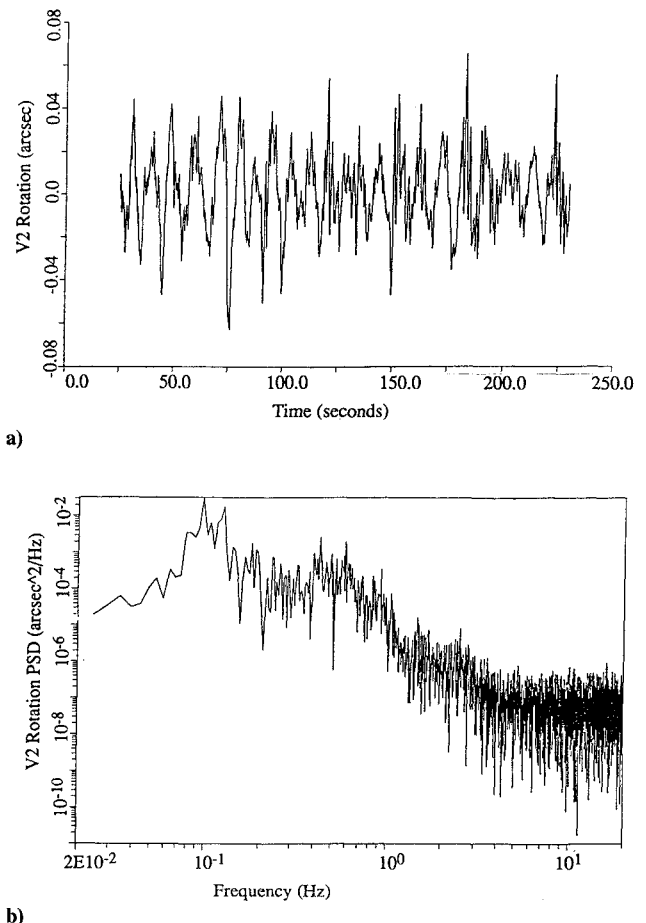


Fig. 9 The  $V_2$  axis pointing error time history and corresponding power spectral density for baseline controller in gyro hold at EON.

installation of SAGA-GA, losses of lock were occurring at approximately 75% of terminators. With SAGA-GA the loss of lock was less than 50%, still undesirably high but an improvement nonetheless.

### SAGA-II

The SAGA-II system was designed to reduce the effects of both the 0.11- and 0.65-Hz SA oscillations on jitter. Goals for the SAGA-II design were stated as follows:

- 1) Maintain a SAGA-GA factor of 30 attenuation at 0.1 Hz.
- 2) Increase attenuation by a factor of 5 over SAGA-GA at 0.65 Hz.
- 3) Maintain adequate stability margins.
- 4) There will be no degradation in gyro hold performance or increase in frequency of loss of fine lock.

On-orbit results have shown that the 0.11-Hz mode is well attenuated with SAGA-GA, so the current factor of 30 was considered sufficient. An improvement much larger than a factor of 5 at 0.65 Hz was unrealistic due to stability limitations (phase loss) of the 40-Hz processing. Stability margins large enough to account for modal uncertainties were required. Finally, although the impulsive nature of large stick-slip disturbances that cause loss of lock made it difficult to predict the effect of the SAGA-II control law, no increase in losses of lock was acceptable.

### Revised Hubble Space Telescope Modal Characteristics

Availability of revised modal data was instrumental in the SAGA-II design; without these data, the new design would not have been possible. This is due to the fact that a refined knowledge of the modes resulted in reduced modal influence coefficients and increased damping. The SAGA-II design appears to be unstable with previous versions of modal data but is adequately stable with the

latest data and is clearly stable on-orbit. Reference 8 discusses the on-orbit modal test known as the concept verification test. Resulting modal characteristics (frequencies, influence coefficients, and damping) are shown in Fig. 2.

### SAGA-II Design

The GA filter for the SAGA-II system is shown schematically in Fig. 10. The filter accommodates up to three sets each of complex poles and zeros. This allowed construction of a notch at 0.11 Hz, a notch at 0.65 Hz, and a pair of poles for rolloff of high-frequency modes. The final frequencies, dampings, and gains were the result of many iterations, examining both the resulting stability margins and disturbance rejection. Figure 10 shows a Bode plot of the GA filter for the  $V_3$  axis.

Table 2 shows open-loop gain crossover frequencies for the baseline PID, SAGA-GA, and SAGA-II systems without bending modes. Bandwidth is increased with SAGA-II but predicted stability margins did not significantly decrease because of improved knowledge of bending mode parameters. Figure 11 shows the Nichols plot for the  $V_3$  axis.

Figure 6 shows the disturbance rejection results for SAGA-II along with the baseline PID and SAGA-GA systems. SAGA-II is seen to have a sharper notch at 0.11 Hz and thus more attenuation exactly at 0.11 Hz but less attenuation on either side. However, the factor of at least 30 is maintained over the required frequencies. At 0.65 Hz, the notch gives a peak attenuation of 10 over the SAGA-

GA system, with attenuation of 5 over the needed range. Although there are frequency ranges where the disturbance rejection is actually degraded when compared to SAGA-GA, the lack of modes to excite at these frequencies means that the impact on jitter is minimal.

Because on-orbit results had shown that the SAGA-GA limiters worked well, they were selected as the baseline set for SAGA-II. A series of simulation runs was performed with the SAGA-II filter, parametrically adjusting the limiters. This work resulted in the final set of SAGA-II limiters only slightly different from the SAGA-GA limiters. These limiters allow the system to degrade gracefully when in the nonlinear operation at terminator crossings.

In addition to frequency-domain stability and disturbance analyses, many simulation runs made with various conditions confirmed performance. Good matches between SAGA-GA simulations and on-orbit results along with improved knowledge of modal parameters led to confidence that SAGA-II performance would be as predicted.

### SAGA-II On-Orbit Results: April 16, 1992 to December 15, 1993

The SAGA-II testing was performed on April 6, 1992. Figure 12 shows annotated strip chart plots of interest from the test. From these plots, it is clear that SAGA-II reduces jitter both during enter orbit day (EOD) terminators and during orbit day. Recovery time at terminators is also reduced with SAGA-II. EON and night periods showed similar improvements.

Figure 13 shows a comparison of power spectral densities (PSDs) for an entire orbit in fine lock. The plots show that attenuation at 0.11 Hz is similar for SAGA-II and SAGA-GA. However, a substantial increase in attenuation is seen at 0.65 Hz. The attenuation factor is computed by taking the square root of the ratio of the PSDs. This shows that attenuation is increased by a factor of 7.5, in excess of the factor of 5 specified, at 0.65 Hz. As expected, attenuation is roughly the same at other frequencies.

On the basis of the successful test, the decision was made to activate SAGA-II for normal operations. This was accomplished on April 16, 1992, and operation to date has confirmed the effectiveness of the SAGA-II control law: jitter is below the 0.007 arc-s over 95% of the time, a significant improvement over the 85% level of SAGA-GA (Fig. 7).

Loss of lock has been linked to the 0.65-Hz disturbances that produce large torques at midday hits. Since SAGA-II attenuates these disturbances, improved loss of lock performance has been realized. The loss of lock percentage at terminators has been reduced by approximately 50%. Correlations with SA angle or time of year are difficult to draw because of the relatively small number of terminators (195 for SAGA-II), but it is clear that SAGA-II reduced the loss of lock rate overall.

### Related Efforts

The latest modification to the HST PCS, known as star recentering, was implemented in January 1993. The recentering algorithm is designed specifically to reduce loss of lock. The algorithm consists of flight software and database changes that couple the HST attitude control law with the fine guidance control system. Recentering blocks inputs from the FGs to the outer (attitude) loop of the control law during short periods during terminators; this complements SAGA-II, which reduces spacecraft jitter by tuning the frequency response of the inner (gyro) loop. Two features of the recentering are FGS star selector servo constraintment and prevention of attitude observer corruption. During recentering, FGS servos are constrained near their nominal "predisturbance" position to prevent wandering caused by erroneous interferometer feedback. Also, FGS updates to the attitude observer are nulled, momentarily placing HST in gyro hold. Recentering is active for approximately 5–15 s during each midday/night disturbance.

Recentering has virtually eliminated loss of lock; occurrences are now rare and are generally attributed to specific "special" events. Since fine lock reacquisitions after loss of lock are time consuming, recentering improves science efficiency.

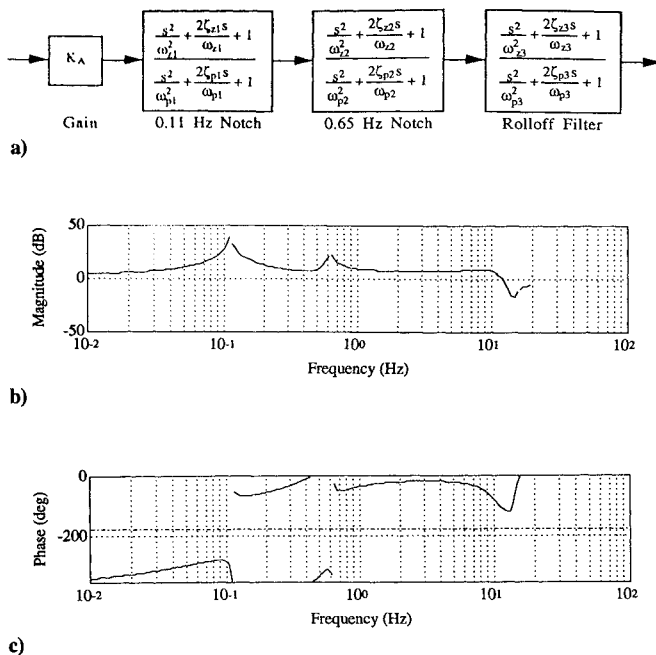


Fig. 10 GA filter and transfer function for SAGA-II.

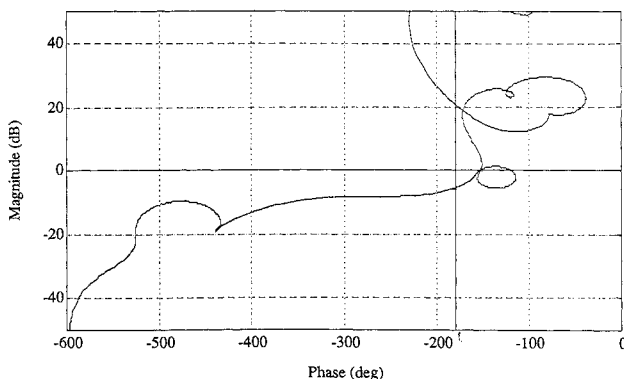


Fig. 11 Nichols plot for  $V_3$  axis with SA at  $90^\circ$  for SAGA-II.

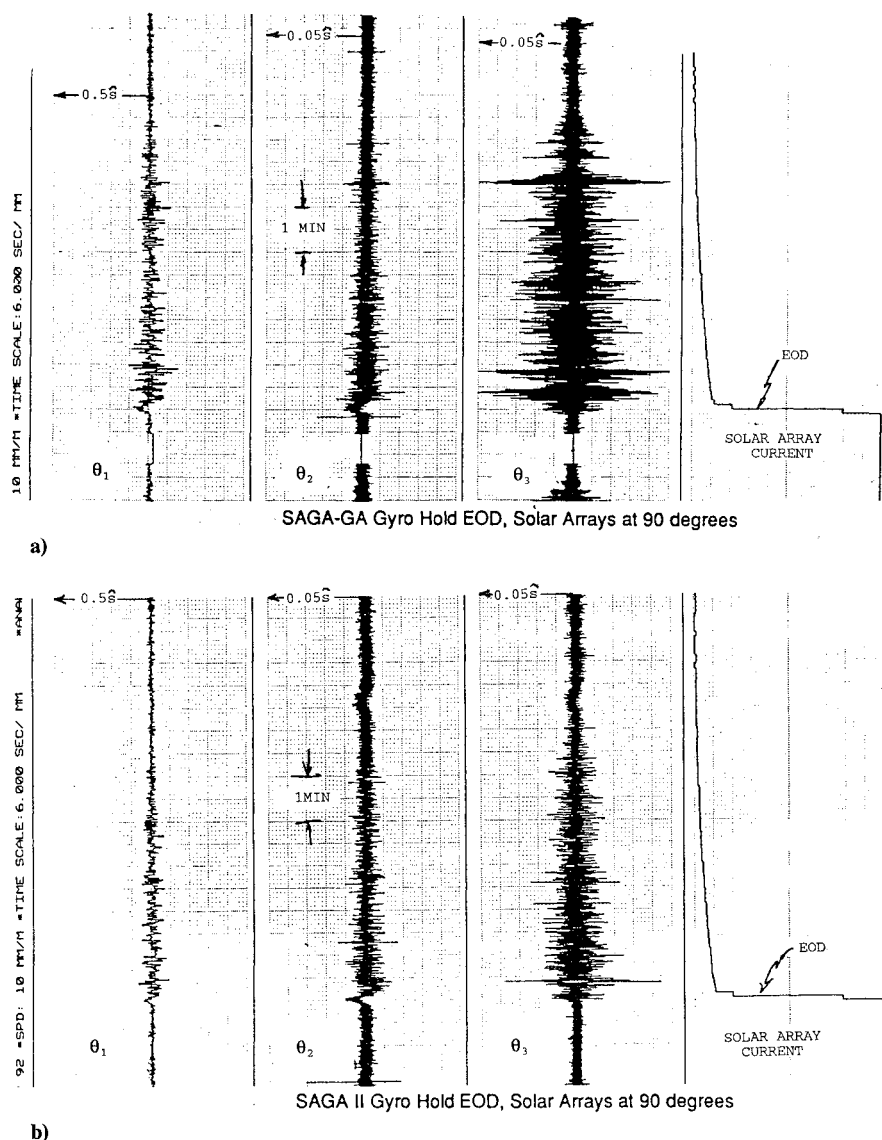


Fig. 12 Strip chart recordings of time history data with SAs at 90° for SAGA-GA and SAGA-II controllers.

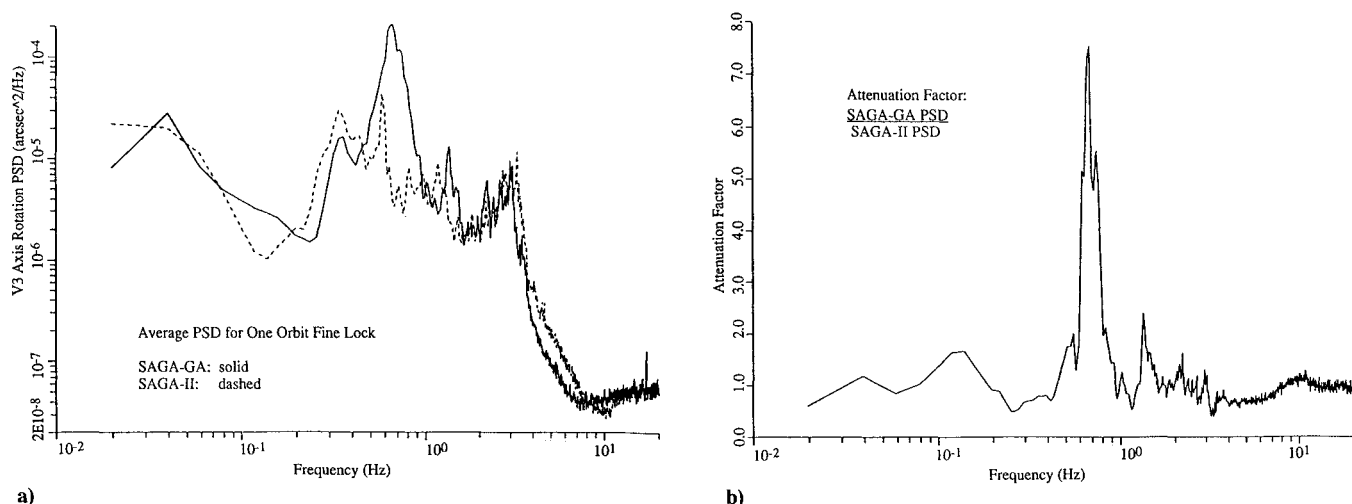


Fig. 13 Comparison of full-orbit PSDs of pointing error for SAGA-GA and SAGA-II.

### Conclusion

The on-orbit SAGA modifications to the HST PCS have allowed satisfaction of the overall pointing stability requirements (0.007 arc-s rms) despite significant thermally driven disturbances from the flexible SAs. The controller bandwidth was increased by approximately a factor of 2, and filters were used to attenuate

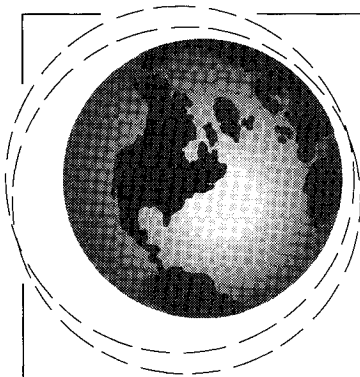
disturbances at the dominant SA modal frequencies of 0.11 and 0.65 Hz by factors of 30 and 10, respectively. The SAGA architecture adds two sixth-order filters to each axis of the baseline vehicle control law. Essential to the success of SAGA is the fact that, despite the limitations of the fixed-point flight computer, the HST hardware and software design was flexible enough to allow these modifica-

tions. The final SAGA-II design was the result of evolution that included an on-orbit transfer function test to reduce uncertainties in the controller design models. Finally, in combination with the complementary software change known as star recentering, modifications to the HST PCS have virtually eliminated guide star loss of lock. These improvements to pointing performance have greatly increased the quantity and quality of preservicing mission science observations of the HST.

During the successful servicing mission in December 1993, modified SAs were installed on the HST. These arrays have significantly reduced the SA disturbances. This was accomplished by covering the bi-stem booms and modifying the array mechanisms to reduce the "slip-stick" phenomena that produce impulsive disturbances. Since the new arrays have bending modes that are somewhat different than the original ones, the SAGA-II controller is no longer in use. Pointing performance with the new SAs and the baseline PID controller is similar to that seen prior to the servicing mission with the SAGA-II controller. An on-orbit transfer function test is planned for the near future to better characterize the modified system dynamics. Following the test, additional tuning of the SAGA controller will be considered in order to reduce jitter even further.

### References

- <sup>1</sup>Fienberg, R. T., "HST: Astronomy's Discovery Machine," *Sky and Telescope*, Vol. 79, No. 4, 1990.
- <sup>2</sup>Nurre, G. S., and Dougherty, H. J., "The Pointing System for Space Telescope," paper presented at Optical Platforms National Symposium and Workshop, June 1984.
- <sup>3</sup>Dougherty, H. J., et al., "Space Telescope Pointing System," *Journal of Guidance, Control, and Dynamics*, Vol. 5, No. 4, 1982, pp. 403-409.
- <sup>4</sup>Nurre, G. S., Anhouse, S. J., and Gullapelli, S. N., "Hubble Space Telescope Fine Guidance Sensor Control System," paper presented at SPIE Conference, March 1989.
- <sup>5</sup>Nurre, G. S., Nelson, J. D., and Bradley, A. J., "Current NASA HST Controller Design and Performance," American Astronautical Society, Paper AAS93-002, Feb. 1993.
- <sup>6</sup>Nurre, G. S., Sharkey, J. P., and Waites, H. B., "Initial Performance Improvement Due to Design Modifications for the Pointing Control System on the Hubble Space Telescope," paper presented at 14th Annual AAS Guidance and Control Conference, Feb. 2-6, 1991.
- <sup>7</sup>Foster, C. L., et al., "The Solar Array-Induced Disturbance of the Hubble Space Telescope Pointing System," paper presented at 61st Shock and Vibration Symposium, Oct. 1990.
- <sup>8</sup>Vadlamudi, N., Blair, M. A., and Clapp, B. R., "Hubble Space Telescope On-Orbit Transfer Function Test," AIAA Paper 92-4614, Aug. 1992.
- <sup>9</sup>Nelson, J. D., "Solar Array Gain Augmentation (SAGA) On-orbit Testing and Performance," Lockheed Missiles and Space Company, Sunnyvale, CA, Engineering Memorandum SPS 613, 11 Jan. 1991.
- <sup>10</sup>Nelson, J. D., "HST SAGA-GA Analysis and Performance," Lockheed Missiles and Space Company, Sunnyvale, CA, Technical Rept., #F420282, 31 May 1992.
- <sup>11</sup>Clapp, B. R., "Transfer Function Concept Verification Test Modal Parameters," Lockheed Missiles and Space Company, Sunnyvale, CA, Engineering Memorandum SPS 634, 28 June 1991.
- <sup>12</sup>Beals, G. A., and Nelson, J. D., Lockheed Missiles and Space Company, Sunnyvale, CA, Engineering Memorandum SPS 663A, 31 January 1992.
- <sup>13</sup>Nelson, J. D., "Solar Array Gain Augmentation (SAGA) On-orbit Testing and Performance," LMSC Rept., EM SPS 613, Jan. 11, 1991.



AIAA Education Series

## Dynamics of Atmospheric Re-Entry

Frank J. Regan and Satya M. Anandakrishnan

This new text presents a comprehensive treatise on the dynamics of atmospheric re-entry. All mathematical concepts are fully explained in the text so that there is no need for any additional reference materials. The first half of the text deals with the fundamental concepts and practical applications of the atmospheric model, Earth's gravitational field and form, axis transformations, force and moment equations, Keplerian motion, and re-entry mechanics. The second half includes special topics such as re-entry decoys, maneuvering re-entry vehicles, angular motion, flowfields around re-entering bodies, error analysis, and inertial guidance.

**AIAA Education Series**  
**1993, 604 pp, illus, Hardback**  
**ISBN 1-56347-048-9**  
**AIAA Members \$69.95**  
**Nonmembers \$99.95**  
**Order #: 48-9(830)**

Place your order today! Call 1-800/682-AIAA



American Institute of Aeronautics and Astronautics

Publications Customer Service, 9 Jay Gould Ct., P.O. Box 753, Waldorf, MD 20604  
 FAX 301/843-0159 Phone 1-800/682-2422 8 a.m. - 5 p.m. Eastern

Sales Tax: CA residents, 8.25%; DC, 6%. For shipping and handling add \$4.75 for 1-4 books (call for rates for higher quantities). Orders under \$100.00 must be prepaid. Foreign orders must be prepaid and include a \$20.00 postal surcharge. Please allow 4 weeks for delivery. Prices are subject to change without notice. Returns will be accepted within 30 days. Non-U.S. residents are responsible for payment of any taxes required by their government.